5th GRACM International Congress on Computational Mechanics
Limassol, 29 June – 1 July, 2005

ULTIMATE STRENGTH ANALYSIS OF ARBITRARY CROSS SECTIONS UNDER BIAXIAL BENDING AND AXIAL LOAD BY FIBER MODEL AND CURVILINEAR POLYGONS

Aristotelis E. Charalampakis and Vlasis K. Koumousis

Institute of Structural Analysis and Aseismic Research
National Technical University of Athens
NTUA, Zografou Campus GR-15773, Athens, Greece
e-mail: vkoum@central.ntua.gr, web page: http://users.ntua.gr/vkoum

Keywords: biaxial bending, fiber model, failure surface, composite structure.

Abstract. *A fiber model algorithm for the analysis of arbitrary cross sections under biaxial bending and axial load is presented. The method can be applied to complex cross sections of irregular shape and curved edges, with or without openings and consisting of various materials. The only assumption is that plane sections remain plane. The cross section is described by curvilinear polygons. The material properties are user – defined; the stress – strain diagrams of all materials consist of any number of consecutive polynomial segments (up to cubic). Various effects such as concrete confinement, concrete tensile strength, strain hardening of the reinforcement etc. may be taken into account. Apart from ultimate strength analyses of cross sections, the algorithm can be applied to other problems in which the Bernoulli – Euler assumption is valid. Based on the proposed algorithm, a computer program with full graphical interface was developed.*

1 INTRODUCTION

The analysis of an arbitrary cross-section under biaxial bending and axial load has received extensive attention in the literature lately [6], [4], [9]. With the advent of inexpensive computer systems, the generation of the failure surface has been made possible using the "fiber" approach. This approach produces consistent results that agree closely with experimental results [2].

The failure of the cross section corresponds to the top of the moment – curvature diagram. However, the conventional failure, defined by design codes, occurs when any of the materials reaches its predefined maximum allowable compressive or tensile strain.

The results of such an analysis are important as they can be used in non-linear analyses of structures where the plastic deformations of a structural element are functions of the load history and the distance of the load vector from the surface. Moreover, it provides grounds for the damage analysis of the cross section.

2 GENERATION OF FAILURE SURFACE

There exist three different techniques to generate the failure surface of an arbitrary cross section: (1) interaction curves for a given bending moments ratio, (2) load contours for a given axial load and (3) isogonic or 3D curves.

The first two techniques require the calculation of the exact position of the neutral axis. The set of equilibrium equations are non-linear and coupled and an iterative approach such as the quasi-Newton method is needed to determine the position of the neutral axis, as proposed by Yen [10]. These procedures are not straightforward to implement and, in many cases, are sensitive to the selection of the origin of the reference system. Moreover, these algorithms usually become unstable near the state of pure compression.

On the other hand, the third technique, which is used in the method presented, is more direct because the direction of the neutral axis is assumed from the very beginning. The produced points describe a more complex 3D plot, because the meridians of the failure surface, in general, are not plane. This is due to the asymmetry of the cross section, as described later.

3 CROSS SECTION

The curvilinear polygon is the only type of graphical entity that is used for the description of all cross sections. A curvilinear polygon has edges that may be straight lines and/or circular arcs. Since these polygons can be nested in any depth, it is obvious that almost any cross section can be described accurately. Circles are taken

into account as two-sided curvilinear polygons with curved edges. Notice that even small objects, such as the reinforcement bars, are treated as actual graphical entities and not dimensionless individual fibers.

In order to significantly reduce the expensive calculations required to identify the various regions in a complex cross section with several materials, each curvilinear polygon is treated separately. Two material properties are defined: the "foreground" material and the "background" material. The foreground material is taken into account with a positive sign, whereas the background material is taken into account with a negative sign. Therefore, almost any cross section can be described, as shown in the example of Figure 1:

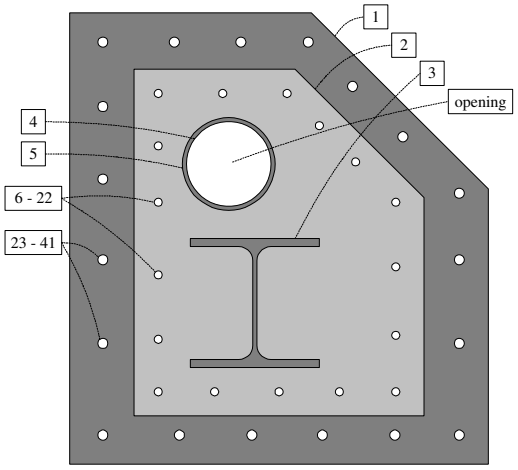

Entity	Number of Nodes	Foreground material	Background material
1	5	Unconfined (outer) concrete	None
2	5	Confined (inner) concrete	Unconfined (outer) concrete
3	16	Structural steel	Confined (inner) concrete
4	2	None	Structural steel
5	2	Structural steel	Confined (inner) concrete
6 – 22	2	Reinforcement	Confined (inner) concrete
23 – 41	2	Reinforcement	Unconfined (outer) concrete

Figure 1. Example of complex cross section consisting of various materials

4 MATERIAL PROPERTIES

The stress – strain diagrams of all materials are composed of any number of consecutive segments. Each segment is a polynomial expression (up to cubic), which is automatically defined by an appropriate number of points; for example, a cubic segment is defined by four consecutive points. Therefore, the stress strain diagrams of a certain kind of concrete and steel may be defined as shown in Figure 2:

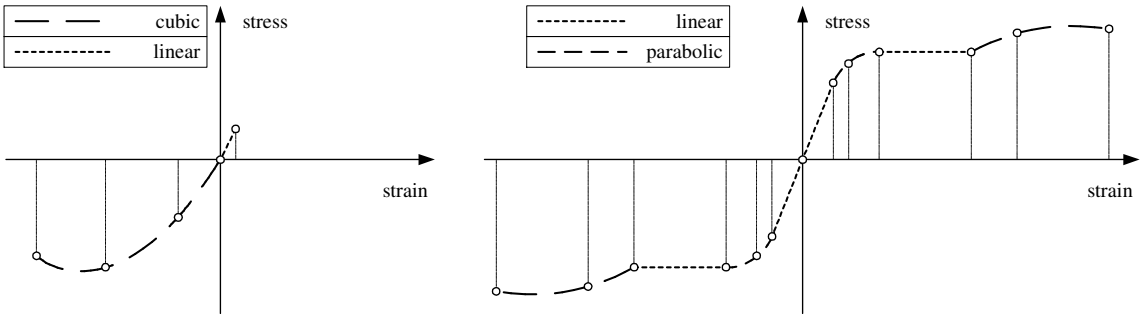

(a) Example of stress - strain diagram (concrete)

(b) Example of stress - strain diagram (steel)

Figure 2. Example of stress – strain diagrams (tension positive)

5 CALCULATIONS

5.1 Rotation

We assume that the X axis is parallel to the central axis of the element. Any convenient point may be used as the origin for the calculations. Since the direction of the neutral axis is assumed from the beginning, it is convenient to express all coordinates in another YZ Cartesian system with Y axis parallel to the chosen direction of the neutral axis. Therefore, the Cartesian system is rotated counter-clockwise around the origin by an angle θ, as shown in Figure 3. In this way, the strains and therefore the stresses vary only in Z axis.

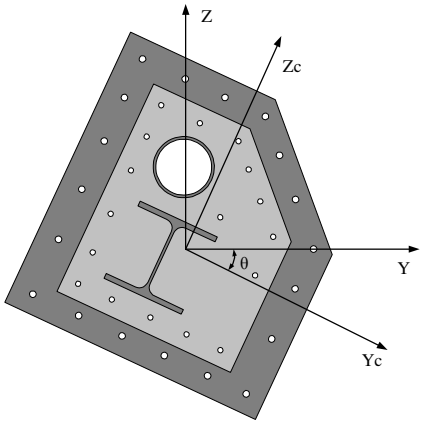

Figure 3. Rotation of cross section

5.2 Decomposition of curvilinear polygons

The next step is the decomposition of all curvilinear polygons into curvilinear trapezoids. The top and bottom edges of the curvilinear trapezoids are straight lines parallel to the neutral axis whereas the left and right edges may be straight lines or arcs. This procedure is required only once for every direction of the neutral axis; this basic set of trapezoids may be stored in memory and retrieved when needed.

Figure 4 shows an example of decomposition of a steel section and some of the produced curvilinear trapezoids. Note that the section is described exactly by a 16-node curvilinear polygon:

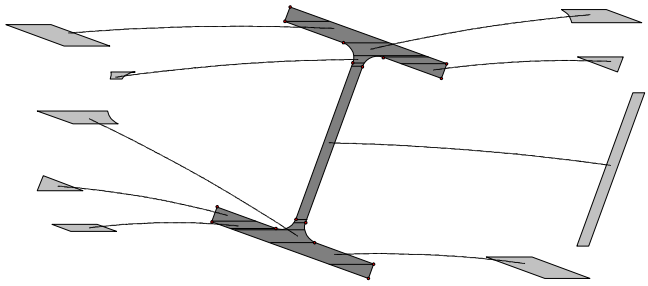

Figure 4. Decomposition of a steel section into curvilinear trapezoids

For reasons of simplicity we will drop the term “curvilinear” for both the curvilinear polygons and the curvilinear trapezoids.

5.3 Calculation of integrals

The next step is the calculation of the basic integrals of the trapezoids. These integrals are of the form $y^m \cdot z^n$, where m, n, are specific integers (equation (1)). All expressions for the integrals are analytical. Again, the integrals need to be evaluated only once for every direction of the neutral axis and the results can be stored in memory for later use. Therefore, the overhead for using analytical expressions is minimal.

$$I^{j}_{(m,n)} = \int_{trapezoid\ j} \left(y^m \cdot z^n \right)$$
$$(m,n) = (0,0..4),\ (1,1..4) \tag{1}$$

This method is also used for the exact calculation of cross sectional properties, such as area, first moments of area, centroids, moments of inertia, products of inertia, principal axes etc.

5.4 Strain distribution

As mentioned before, the main assumption is that plane sections remain plane. Therefore, three parameters are needed to define the deformed plane, namely the direction of the neutral axis (angle θ), the curvature k and the strain ε_0 at the origin, as shown in Figure 5:

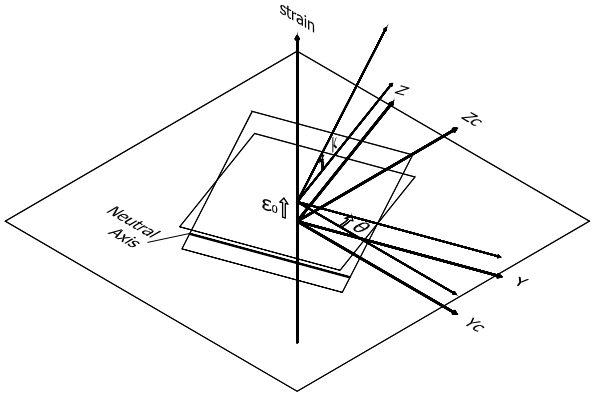

Figure 5. Deformed plane (expressed in terms of strains)

Since the Cartesian system has been rotated by an angle θ, the strain is a function of z only (equation (2)):

$$\varepsilon(z) = \varepsilon_0 + k \cdot z \tag{2}$$

Given k, ε_0, the neutral axis is defined as the line parallel to the Y axis at a distance given by equation (3):

$$z_{na} = -\frac{\varepsilon_0}{k} \tag{3}$$

5.5 Calculation of stress resultants

The calculation of stress resultants will take place for an imposed deformed configuration defined by a set of given values of the parameters θ, k, ε_0. In general, we assume that the segment of the stress – strain diagram covering the specific trapezoid is a cubic polynomial expression of the following form:

$$\sigma(\varepsilon) = \sum_{i=0}^{3}\left(a_i \cdot \varepsilon^i\right) \tag{4}$$

The coefficients α_i are known from the properties of the material. Substituting relation (2) into (4) we obtain:

$$\begin{aligned}
&\sigma(k, \varepsilon_0, z) = \sum_{i=0}^{3}\left(b_i \cdot z^i\right) \\
&b_0 = \alpha_3 \cdot {\varepsilon_0}^3 + \alpha_2 \cdot {\varepsilon_0}^2 + \alpha_1 \cdot \varepsilon_0 + \alpha_0 \\
&b_1 = 3 \cdot \alpha_3 \cdot {\varepsilon_0}^2 \cdot k + 2 \cdot \alpha_2 \cdot \varepsilon_0 \cdot k + \alpha_1 \cdot k \\
&b_2 = 3 \cdot \alpha_3 \cdot \varepsilon_0 \cdot k^2 + \alpha_2 \cdot k^2 \\
&b_3 = \alpha_3 \cdot k^3
\end{aligned} \tag{5}$$

The stress resultants of trapezoid j are calculated by integration of equation (5) as:

$$N_x^j = \int_{trapezoid\ j}\left(\sum_{i=0}^{3}\left(b_i \cdot z^i\right)\right) = \sum_{i=0}^{3}\left(b_i \cdot \int_{trapezoid\ j}\left(z^i\right)\right) = \sum_{i=0}^{3}\left(b_i \cdot I_{(0,i)}^j\right) \tag{6}$$

$$M_y^j = \int_{trapezoid\ j}\left(\sum_{i=0}^{3}\left(b_i \cdot z^i\right) \cdot z\right) = \sum_{i=0}^{3}\left(b_i \cdot \int_{trapezoid\ j}\left(z^{i+1}\right)\right) = \sum_{i=0}^{3}\left(b_i \cdot I_{(0,i+1)}^j\right) \tag{7}$$

$$M_z^j = \int_{trapezoid\ j}\left(\sum_{i=0}^{3}\left(b_i \cdot z^i\right) \cdot y\right) = \sum_{i=0}^{3}\left(b_i \cdot \int_{trapezoid\ j}\left(z^i \cdot y\right)\right) = \sum_{i=0}^{3}\left(b_i \cdot I_{(1,i)}^j\right) \tag{8}$$

Note that the integrals $I_{(m,n)}^j$ have already been calculated and are independent of k, ε_0. By a simple summation of the stress resultants of all trapezoids, the overall forces and bending moments required to impose

the specific deformed configuration are obtained. Therefore, the steps to calculate the stress resultants are as follows:

- Pick k, $\varepsilon_{0.}$
- For trapezoid j:
  Calculate b_i as functions of α_i (equations (5))
  Calculate the stress resultants using the known values of $I_{(m,n)}^{j}$ (equations (6) to (8)).
- Sum the results from all trapezoids to obtain overall stress resultants N_X, M_Y, M_Z.

6 CONSTRUCTION OF MOMENT-CURVATURE DIAGRAM

For a specified axial load and direction of neutral axis (angle θ), a full moment – curvature diagram can be constructed. After the initialization (rotation of cross section, decomposition of polygons into trapezoids, calculation of the basic integrals of the trapezoids), small increments of Δk are applied as imposed curvature. Since θ, k are given, the deformed plane is only a function of strain ε_0 at the origin. The algorithm calculates an upper and lower bound of ε_0 and uses a fast Van Wijngaarden – Dekker – Brent method to calculate ε_0 in order to achieve axial equilibrium to a specified accuracy.

As the curvature increases, the neutral axis moves perpendicular to its direction. This incremental procedure continues until the moment reaches a maximum (failure), or until one of the materials reaches the maximum compressive or tensile strain specified by the user (conventional failure). Thus, the complete moment – curvature diagram can be obtained, both for the primary moment M_Y and for secondary moment M_Z. In general, the secondary moment M_Z, expressed by equation (8), is small as compared to the primary moment M_Y. Finally, the moments can be expressed in the global reference system with an inverse rotational transformation.

The algorithm uses a variable curvature step which is adjusted automatically; therefore, the final result is independent of the initial curvature step (specified by the user). A small initial curvature step produces a smooth moment – curvature diagram.

7 CONSTRUCTION OF INTERACTION CURVES AND FAILURE SURFACES

By repeating the procedure described previously for different directions θ of the neutral axis in the range of 0^0 – 360^0, we are able to construct the interaction curve for a given axial load. In addition, by constructing interaction curves for various axial loads, we are able to construct the full failure surface of the cross section equator – by – equator.

8 DEFORMED CONFIGURATION UNDER GIVEN LOADS

The algorithm can also be used for calculating the deformed configuration of a cross section under given loads. The calculation is a trial and error procedure (Figure 6). The task is to calculate the parameters θ, k, ε_0 of the deformed plane for which the cross section is in equilibrium with the external loads N_{Xc}^{T}, M_{Yc}^{T}, M_{Zc}^{T}.

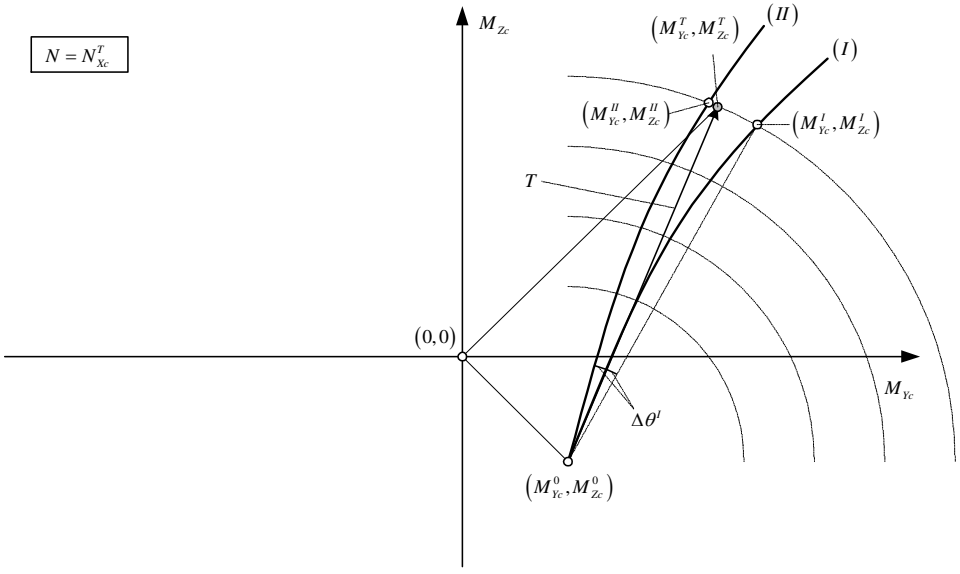

Figure 6. Calculation of deformed configuration under given loads

All calculations are performed with axial load equal to N_{Xc}^{T}. The origin can be any point; therefore, we first have to calculate the bending moments M_{Yc}^{0}, M_{Zc}^{0} required for a deformed plane with no curvature (k=0). Since curvature is always increased from zero until failure, this bending moment vector is the first result for any direction θ of the neutral axis. Therefore, the paths of all analyses stem from (M_{Yc}^{0}, M_{Zc}^{0}). The target vector T connects (M_{Yc}^{0}, M_{Zc}^{0}) with (M_{Yc}^{T}, M_{Zc}^{T}).

As first attempt (I), we set the direction θ^{I} of the neutral axis equal to the direction of the target vector T. As curvature is increased, the path of the analysis deviates because of the secondary moment M_Z; when the norm reaches the norm of the target vector, the analysis stops and the result (M_{Yc}^{I}, M_{Zc}^{I}) may differ from the target values (M_{Yc}^{T}, M_{Zc}^{T}). The direction of the neutral axis is then corrected by the difference $\Delta\theta^{I}$ found in the first iteration. In the second attempt, the results (M_{Yc}^{II}, M_{Zc}^{II}) are much closer to the target values. The procedure stops when a specified accuracy is achieved.

8 COMPUTER IMPLEMENTATION

A computer program, called myBiAxial, which implements the method proposed, has been developed. The program features a full graphical interface. Some screen shots are shown in Figure 7:

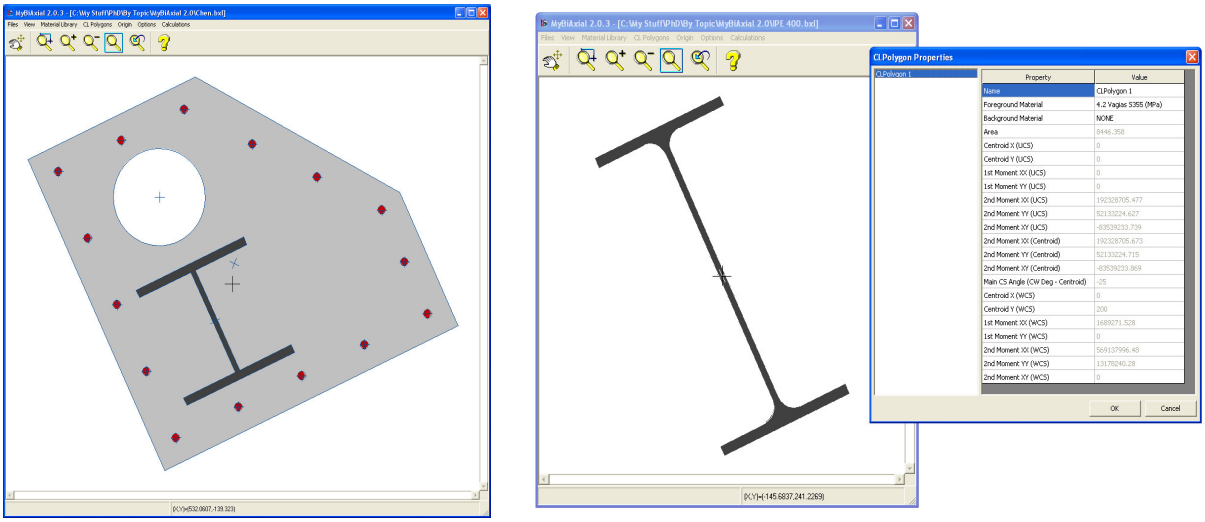

(a) (b)

Figure 7. MyBiAxial computer program

9 VALIDATION - EXAMPLES

9.1 Example 1

Eurocode 2 provides design charts for common reinforced concrete cross sections. These charts provide combinations of axial loads and their respective ultimate bending moment capacities for a range of longitudinal reinforcement expressed by the mechanical reinforcement percentage ω.

The axial load and bending moment are in a non-dimensional form with respect to the concrete properties and the cross sectional dimensions; therefore, a single chart covers all cases for a certain steel grade.

Eurocode 2 specifies the value of 0.020 as the ultimate strain limit for longitudinal steel reinforcement. Also, for large compressive axial loads, it reduces the ultimate curvature capacity by imposing the rotation of the strain profile around point C which is located at a distance 3/7·h from the most compressed fiber and has a strain of ε_0=-0.002. This restriction is included easily in the algorithm; however, it is of little practical interest since large compressive axial loads in concrete cross sections must be avoided for other reasons i.e. creep.

The developed computer program was used to calculate pairs of axial loads and bending moments for the rectangular cross section of Figure 8a. The characteristic strengths and partial safety factors for concrete and reinforcement bars were taken as follows: f_{ck}=20MPa, γ_c=1.5, f_y=500MPa, γ_r=1.15.

Five different cases of longitudinal reinforcement were considered, i.e. ω=0.00, 0.50, 1.00, 1.50, 2.00. The computed results follow the corresponding curve exactly, as shown in Figure 8c.

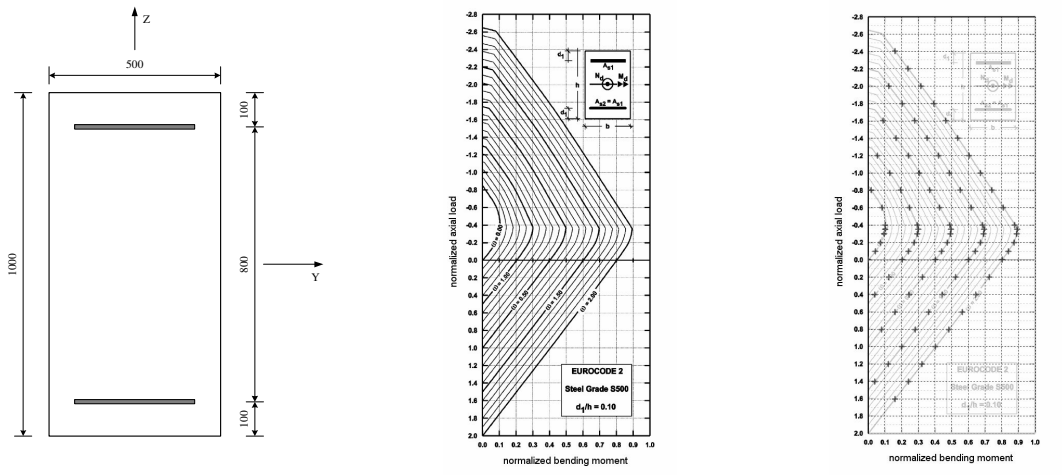

(a) (b) (c)

Figure 8. (a) Rectangular reinforced concrete cross section (distances in mm) (b) Corresponding EC2 design chart (steel grade S500) (c) Results from proposed algorithm superimposed over the design chart

9.2 Example 2

This is an example presented by Chen et al. [2], which invokes the polygonal composite column cross section of Figure 9. The cross section consists of a concrete core, an asymmetrically placed H – shaped steel section, 15 reinforcement bars of diameter 18mm and a circular opening.

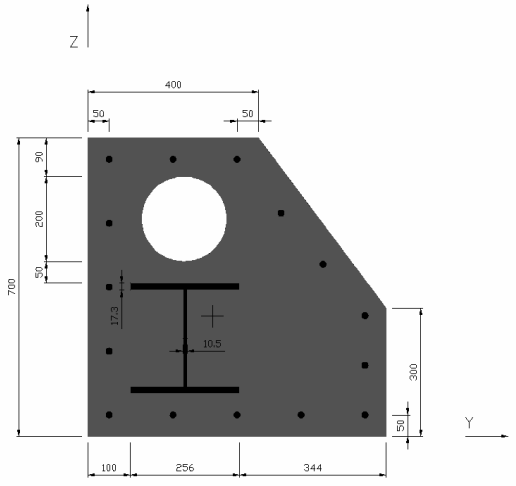

Figure 9. Composite column cross section

Chen et al. use a quasi – Newton method [10] to analyze the cross section. However, the convergence of the iterative process invoked by this algorithm cannot be guaranteed when dealing with large axial loads i.e. loads that approach the axial load capacity under pure compression. In order to ensure the stability of Chen's algorithm, the plastic centroid must be used as the origin of the Cartesian system. In this case, the coordinates of the plastic centroid with respect to the bottom left corner are [2] Y_{pc}=292.2mm, Z_{pc}=281.5mm.

The stress – strain curve for concrete (CEC 1994) which consists of a parabolic and a linear (horizontal) part was used in the calculation, with $f_{cc}=0.85\cdot f_{ck}/\gamma_c$, ε_0=0.002 and ε_{cu}=0.0035. The Young modulus for all steel sections was 200GPa while the maximum strain was $\varepsilon_u=\pm 0.010$. The characteristic strengths and partial safety factors for concrete, structural steel and reinforcement bars were taken as follows: f_{ck}=30MPa, γ_c=1.5, f_s=355MPa, γ_s=1.1, f_y=460MPa, γ_r=1.15. The analysis was carried out with an angle step of 5 degrees and an initial curvature step of 1e-05.

Figure 10a shows the interaction curve produced by the proposed algorithm for compressive axial load 4120kN. The image is superimposed over the results taken from [2]; it is obvious that the curves almost coincide.

The same figure also shows the paths of the analyses and the directions of the neutral axes that correspond to each spike. Note that the data for each spike becomes denser near failure; this is because the curvature step is decreased in order to achieve accuracy. By repeating this procedure for various axial loads we obtain the complete failure surface of Figure 10b.

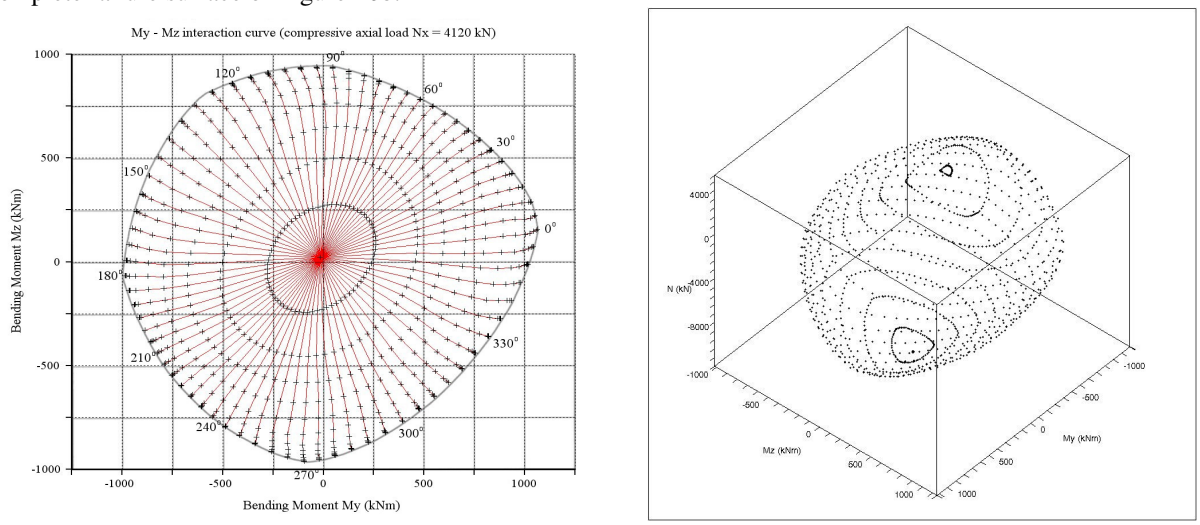

(a) (b)

Figure 10. (a) Interaction curve for compressive axial load 4120 kN (b) Complete failure surface

10 CONCLUSIONS

A generic algorithm for the analysis of arbitrary cross sections under biaxial bending and axial load is presented. The algorithm has some unique features as compared to the literature. The cross section is described by curvilinear polygons, i.e. closed polygons with straight or curved edges; the material stress – strain diagrams are fully user – defined as piecewise functions of polynomial segments; the integration of the stress field is analytical. Apart from producing interaction curves and failure surfaces, the algorithm can be used for the calculation of the deformed state of the cross section under given loads.

The algorithm has proved to be very stable and fast, while providing accurate results for non-linear analysis.

REFERENCES

[1] Bonet, J.L., Romero, M.L., Miguel, P.F., Fernandez, M.A. (2004), "A fast stress integration algorithm for reinforced concrete sections with axial loads and biaxial bending", Computers and Structures 82 213-225

[2] Chen, S. F., Teng, J. G., Chan, S. L. (2001), "Design of biaxially loaded short composite columns of arbitrary cross section", J. Struct Engng, ASCE; 127(6):678-685.

[3] De Vivo, L, Rosati, L. (1998), "Ultimate strength analysis of reinforced concrete sections subject to axial force and biaxial bending", Comput. Methods Appl. Mech. Engrg. 166:261-287.

[4] Fafitis, A (2001), "Interaction surfaces of reinforced-concrete sections in biaxial bending", J Struct Engng, ASCE; 127(7):840-6

[5] Press, W. H., Teukolsky, S. A., Vetterling, W. T., Flannery, B. P. (2002), *Numerical recipes in C++: the art of scientific computing*, Cambridge University Press.

[6] Rodriguez, J. A., Aristizabal-Ochoa, J. Dario (1999), "Biaxial interaction diagrams for short RC columns of any cross section", J Struct Engng, ASCE; 125(6):672-683.

[7] Rodriguez, J. A., Aristizabal-Ochoa, J. Dario (2001), "M-P-φ diagrams for reinforced, partially and fully prestressed concrete sections under biaxial bending and axial load", J Struct Engng, ASCE; 127(7):763-773.

[8] Rodriguez, J. A., Aristizabal-Ochoa, J. Dario (2001), "Reinforced, partially and fully prestressed concrete columns under biaxial bending and axial load", J Struct Engng, ASCE; 127(7):774-783.

[9] Sfakianakis, M. G. (2002), "Biaxial bending with axial force of reinforced, composite and repaired concrete sections of arbitrary shape by fiber model and computer graphics", Advances in Engineering Software 33 227 - 242.

[10] Yen, J. Y. R. (1991), "Quasi-Newton method for reinforced concrete column analysis and design", J Struct Engng, ASCE; 117(3):657-666.